Suffolk University

Suffolk University

Astrophysics Senior Project

Study of OH/IR stars in the galactic bulge using Virtual Observatory methodologies

Authors:
Jorge Bernal & Zoe Wells

Supervisor:
Francisco Jiménez Esteban

December 2013

Contents

1 Abstract **1**

2 Introduction **1**
2.1 AGB stars 1
2.2 Virtual Observatory 2

3 The sample **2**

4 Analysis **3**
4.1 Spectral energy distribution 3
4.2 Bolometric fluxes and luminosities 4
4.3 Variablity 5

5 Results and Conclusion **6**

6 Acknowledgement **13**

Index of tables

1 These objects had irregular SEDs and could not be classified. 3
2 Objects shown with their candidacy classification, their model fit, bolumetric luminosity, mean magnitude (K), the difference in filter magnitude (ΔK), and difference in time (Δt). Objects with an ($*$) are highly promising AGB candidates. 6

List of Figures

1 Bad SED fit to model. 4
2 Good SED fit to model. 5
3 Luminosities of the galactic bulge sample. 5

1 Abstract

Context: The asymptotic giant branch (AGB) of stellar evolution continues to be poorly understood, even though it is the fate of thousands of stars including our own Sun. There are various questions that remain unanswered about this branch. Many are related to the mass-loss process, luminosity of the star within the circumstellar envelope, and the relation between the progenitor-mass and the maximum mass-loss rate.
Aims: To study a sample of AGB sources within the galactic bulge for further analysis.
Methods: Using Virtual Observatory data and tools to analyze OH maser sources for variability, and their spectral energy distribution. we identified those sources that were likely AGB stars. By using galactic bulge sources we assume a common distance and we can later analyze our selected sample for individual interstellar extinction, luminosity and infer the progenitor-mass range using theoretical models.
Results: We classified 151 objects as possible AGB candidates based on their fit to the GRAMS model, 25 of which had variability data that allowed us to classify them as highly promising AGB candidates.

2 Introduction

2.1 AGB stars

The asymptotic giant branch (AGB) is the final evolutionary phase for stars with masses between $1M_{\odot}$ to $8M_{\odot}$ and it is after this phase that these stars create planetary nebulae and white dwarfs. This stage of evolution is after a red giant star has experienced central He-burning and the horizontal branch and lasts for $\leq 1\%$ of the total lifetime of the star. This is the phase where these cool, red giants reach maximum luminosity, which makes them easier to observe (Engels 2005). At this phase the star has produced a circumstellar envelope (CSE).

AGB stars are a part of a class of objects known as OH/IR sources. These are sources that give off OH maser emissions and produce most of their energy in infrared frequencies. It is with this strong infrared radiation and the variability of the TP-AGB stars that they are more easily identified. The inner region of the star consists of a degenerate C-O core, surrounded by a He-burning shell, and an H-burning shell. The CSE is made by a large mass loss and consists of dust and gas particles (Olofsson 1999).

There are two evolutionary stages on the AGB, early AGB (E-AGB) and thermal pulse AGB (TP-AGB). The E-AGB occurs when the He-burning shell is producing most of the energy output. Eventually the H-burning shell reignites and becomes the main energy source. However; the H-burning shell produces He that falls back into the He shell below. With this increases of mass, when the temperature of the He shell increases enough there will be a He shell flash. This flash results in a large energy release and causes the H-burning shell to move outward, cool and turn off. Eventually the He-burning shell cools and the H-burning shell reignites and the process restarts. These He shell flashes cause a sudden decrease in the stars surface luminosity and provide quasi-periodic variability.

The flash can also cause a convection zone between the He-burning and the H-burning shells,

where carbon can be made. However; depending on the mass of the star, the nuclear reactions that happen within dictate the chemistry of the star. There are three postulated chemical branches of AGB stars. The first is a low-mass oxygen-rich star which has too little mass for the third dredge-up to occur. The third dredge-up is when the convection zone extends deeper into the star and the carbon-rich material is pushed to the surface of the star, changing the surface chemistry and oxygen to carbon ratio of the star. The intermediate-mass stars, which have had their dominant chemistry changed after several thermal pulses due to the third dredge up. Lastly, in more massive stars the third dredge-up and hot bottom burning can happen. Hot bottom burning is when the convection zone extends more deeply into the star and collects more material from the burning shell. This means that the bottom of the convective zone is actually undergoing nuclear burning itself. It is during the TP-AGB phase that much of the remaining mass of the star is lost due to nuclear burning and He flashes. By the end of the TP-AGB there is barely more than the C-O core of the star.

2.2 Virtual Observatory

Using Virtual Observatory (VO) data and tools we were able to analyze a sample of 309 OH maser sources within the Galactic Bulge, defined as $|10\,^{\circ}|$ of the Galactic Center and identified 295 of them as possible AGB candidates. The VO is an archive of astronomical data sets and surveys, and the necessary tools to use this data available for use by astronomers around the globe. By utilizing the VO data and tools we were able to conduct research and analysis in a shorter period of time. We used topcat, to manipulate data tables and cross matches, Aladin, for visual image checks.Lastly, we used the Virtual Observatory SED Analyzer (VOSA), which generates spectral energy distribution (SED) graphs.

3 The sample

Our selection of the sample of OH/IR stars in the Galactic Bulge started with the three catalogs of sources produced in The ATCA/VLA OH 1612 MHz survey by Sevenster et al.(Sevenster et al. 1997;Sevenster et al. 2001). The collected data was presented in three papers and catalogs divided by the regions of the sky that was surveyed. The first region was the Galactic Bulge region; which is defined as $|10\,^{\circ}|$ latitude and $|3\,^{\circ}|$ longitude of the Galactic Center. The second region was the Galactic Disk region; which is defined as $-45\,^{\circ}$ to $-10\,^{\circ}$ latitude and$|3\,^{\circ}|$ longitude of the Galactic Center. The last region was the Northern Galactic Plane, which is defined as $5\,^{\circ}$ to $45\,^{\circ}$ latitude and $|3\,^{\circ}|$ longitude of the Galactic Center. In total this survey collected 766 OH maser sources, of single peak, double peak and irregular spectral profiles.

The goal of our study is to analyze AGB stars in the Galactic bulge region, thus from the 766 sources provided by the survey we selected our starting sample using their galactic coordinates. Using the definition of the Galactic Bulge as within $|10\,^{\circ}|$ of the Galactic Center, we took only sources within that range. This yielded 309 sources, from which we removed any sources denoted as irregular by the survey or having an expansion velocity (VE) higher than 30 km s^{-1}, as they are likely not AGB stars. After that reduction of data our sample list contained 303 sources from the original survey.

4 Analysis

4.1 Spectral energy distribution

That list was then cross matched with the following virtual observatory catalogs: the WISE catalog at 3.56, 4.51, 5.76, and 22.1 m (filters W1, W2, W3, and W4, respectively); GLIMPSE at 3.56, 4.51, 5.76, and 7.96 m (filters I1, I2, I3, and I4, respectively); MSX6C Infrared Point Source Catalog at 8.28, 12.13, 14.65, and 21.3. m (filters A, C, D, and E, respectively), IRAS Point Sources Catalog at 12, 25, 60, and 100 m (fiters 12, 25, 60, and 100, respectively); AKARI Point Source Catalog at 9, 18, 65, 90, 140, and 160 m. This was to collect photometric data to construct the SED. We used a search radius of 3.0 arcseconds for the WISE catalog, 2.5 arcseconds for GLIMPSE, 10.0 arcseconds for MSX6C, 35.0 arcseconds for IRAS, and 34.0 arcseconds for both AKARI catalogs. The next step was removing magnitude or flux measurements that did not also have values in error of the measurements for that filter. This was to ensure only reliable photometric data was used to build our SEDs. ** from the WISE catalog (Wright et al. 2010), GLIMPSE (Churchwell et al. 2009), MSX6C Infrared Point Source Catalog (Egan et al. 2003), IRAS Point Sources Catalog (Beichman et al. 1988), and the AKARI Point Source Catalog (Ishihara et al. 2010; Yamamura et al. 2010). **

Table 1: These objects had irregular SEDs and could not be classified.

Object	Class	Chi2	Lbol
OH000.207+01.414	I	1877.616	5334.377
OH000.344+01.567	I	4158.886	12311.68
OH001.095-00.832	I	178.8597	1749593
OH003.078-00.027	I	509.7974	6168.824
OH003.203+00.024	I	4317.687	1491.661
OH004.376+00.122	I	228.5131	4363.07
OH005.885-00.392	I	219.7875	1403286
OH350.546+00.061	I	4857.585	5909.886
OH351.474-00.596	I	626.2407	6604.061
OH354.509-01.377	I	11927.96	5297.883
OH354.647-00.182	I	1039.729	28976.92
OH355.111-01.697	I	41865.92	7061.351
OH359.233-01.876	I	3767.227	15074.1
OH359.938-00.052	I	770.2706	5736653

Once all of the cross matched tables were edited to have only data with reliable photometry we converted the magnitude values from the WISE and GLIMPSE tables into fluxes. The AKARI, IRAS, and MSX6C data was already measured in fluxes. When all of the data and errors had been converted into $\mathrm{erg\,s^{-1}\,cm^{-2}\,\AA^{-1}}$ we compiled a table that had all of the original Sevenster data and the flux and error values from all of the catalogs.

When uploaded to VOSA, the objects were given parameters to refine their SEDs. Their distance from Earth was set to 8 kpc, the distance to the Galactic Center with an error of 1.41 kpc corresponding to the $|10^{circ}|$ radius of our sample. We also added interstellar extinction range between 0 and 30.0 (Av: 0.0/30.0). Table 1 shows the 14 objects with irregular SEDs

were removed after fitting them to the model.

4.2 Bolometric fluxes and luminosities

Once the SEDs were constructed in VOSA, they were fit to the GRAMS (Grid of Red supergiant and Asymptotic giant Modes) **Reference**, a grid of radiative transfer (RT) models for dust shells around red supergiant (RSG) and asymptotic giant branch (AGB) stars. This is the model grid used for Oxygen-rich AGBs. Fig. 1 and Fig. 2 show a bad and a good SED fit to the GRAMS model respectively. VOSA was unable to make fits for 14 of the objects, as they lacked enough data points. The remaining 281 fits were analyzed. Based on the 8 kpc distance of the Galactic Center, the theoretical luminosity limit of an AGB star was assumed to be $6.0 * 10^4 L_{\odot}$ with an error of $2.1 * 10^4 L_{\odot}$. This was used to identify foreground and non-AGB sources. Fig. 3 shows a histogram of the luminosities calculated by VOSA of the Galactic Bulge Sample near the AGB luminosity limit.

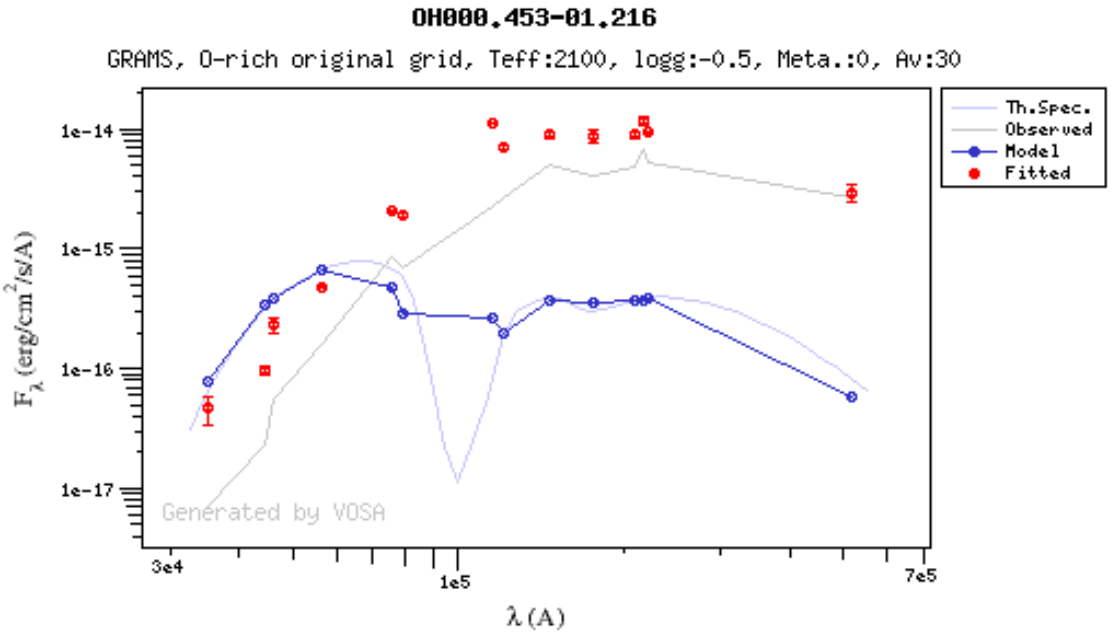

Figure 1: Bad SED fit to model.

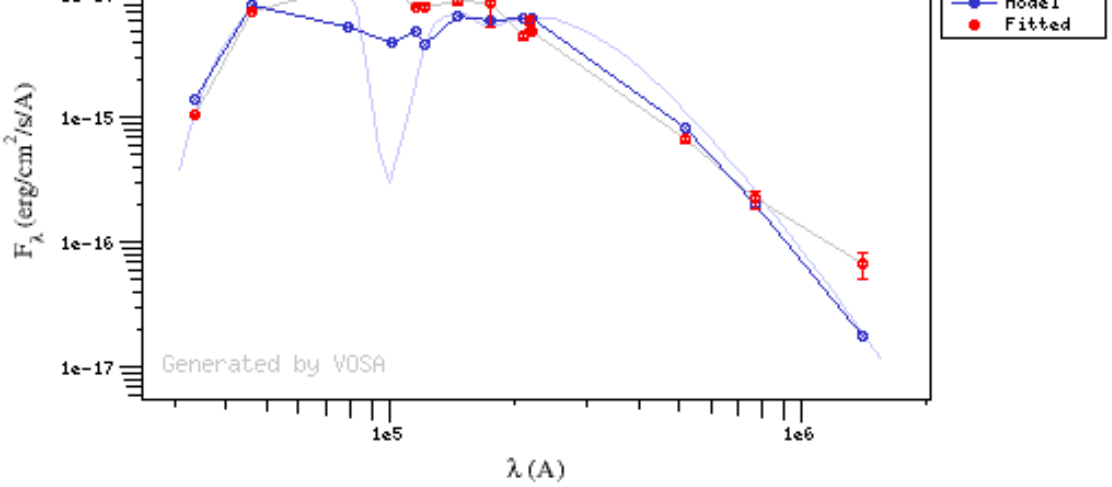

Figure 2: Good SED fit to model.

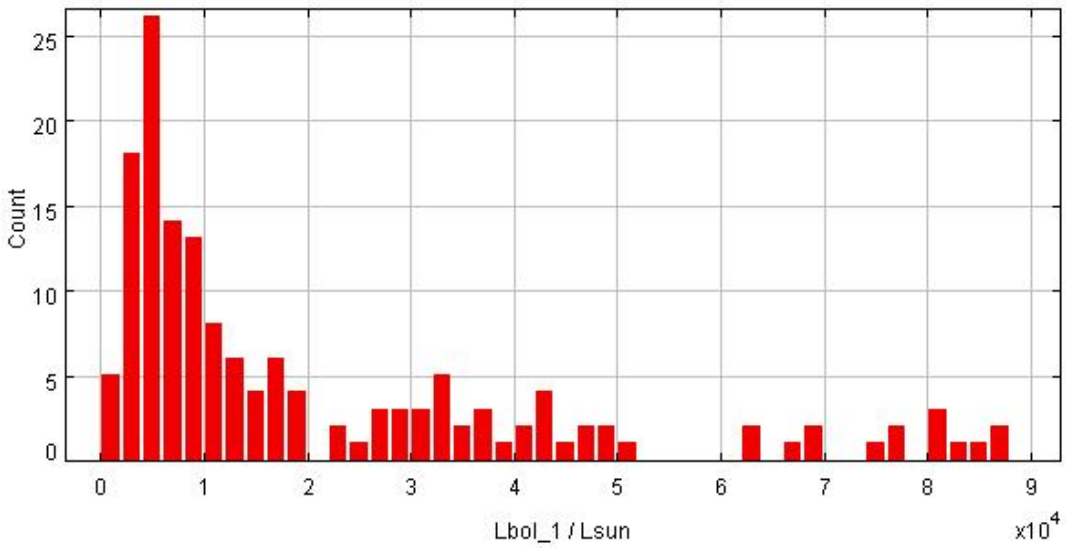

Figure 3: Luminosities of the galactic bulge sample.

4.3 Variablity

Along with visually analyzing each source's SED, we also checked the variability of the source to confirm it as an AGB. This was done by writing a program that read in different measurements of the sources magnitude provided by VISTA. These were measurements that were taken using different frequency filters at different times. Our program read all of the measured magnitude values of one source, then subset the data based on what filter was used for the measurement. From there the mean value for the K filter measurements was produced. As many of the measurements would occur on the same day, the mean value for each observation day also had to be found. The minimum and maximum mean magnitudes were produced for each source from the difference days of measurement, and the difference provided the amplitude of the photometric variability. The difference of the days that these measurements were taken was also calculated. Since AGB stars are known to be large amplitude variable stars, if the amplitude was less than 0.2 then the source was flagged as not having the data to confirm it as an AGB star.
Using the data provided by this program we could see the variability of the source and the time

of that variability. This data, along with the SEDs provided by VOSA were used to identify which of our sources were AGB stars.

5 Results and Conclusion

The luminosities of the AGB candidate objects range from $373L_{\odot}$ to $7*10^{6}L_{\odot}$, with one object, OH352.625+03.014, having a luminosity of $2*10^{7}L_{\odot}$. Objects with AGB candidate SEDs whose luminosity is above the calculated AGB limit of $6*10^{4}L_{\odot}$ may come from our calculation of the Galactic Bulge Sample being at a distance of 8kpc. Their high luminosities suggest they are foreground objects between us and the limits of our definition of the galactic bulge. Accounting for error in the luminosity calculations, there are 151 objects classified as AGB candidates that are below the AGB luminosity limit. The classification chosen for visual classification was either AGB candidate, Post-AGB candidate, foreground object or non-AGB, or Irregular (A, P, F, and I, respectively) using the SED. Of these, three pairs of objects (OH008.885-00.56 and OH008.885-00.517, OH008.933-00.014 and OH008.933-00.015, and OH009.334+00.129 and OH009.335+00129) had the same SED and model fit, suggesting they come from the same source.

The data from the VISTA catalog that we used to test for variability was limited but generally had at least one day of measurements for our sources. This helped us confirm that our source was at these coordinates. This data had errors in measurement for some objects, made apparent by their measured magnitudes of $-1.0*10^{9}$, these data points were ignored during the analysis, but are noted on the final table. Based on the data that had multiple days of observation in the K filter, 25 out of the 148 candidate sources were considered highly promising AGB candidates The data was considered promising when the amplitude was higher than 0.2 and measured time different greater than 10 days. However, while this data supports candidacy of some objects, it is not enough to discount any sources.

Table 2: Objects shown with their candidacy classification, their model fit, bolometric luminosity, mean magnitude (K), the difference in filter magnitude (ΔK), difference in time (Δt), and number of measurements. Objects with an ($*$) are highly promising AGB candidates.

Object	**Class**	χ^2	**Lbol($L_{\odot}$)**	**K(mag)**	**ΔK(mag)**	**Δt(Days)**	**Meas**
OH000.000+00.352	A	127.53645	46865.84	no data			0
OH000.024-00.874	A	144.53752	4751.182	9.7273	0.9078	136.7069	39
OH000.071-00.205	A	368.7349	6832.727	13.6925	0	0	3
OH000.072-02.044	P	1221.9155	3254.39	9.0835	0	0	12
OH000.190+00.036	A	306.56326	18319.81	12.4344	0	0	3
OH000.207+01.414	I	1877.6155	5334.377	13.064	0.1285	7.0913	6
OH000.260+01.027	A	1219.8477	13248.76	10.2745	0.30477	6.1324	8
OH000.313+01.674	A	13.032989	17584.36	9.2533	2.3865	6.1328	5
OH000.319-00.041	A	866.4879	4305.645	15.8587	0	0	1
OH000.333-00.181				14.8623	0	0	4

OH000.344+01.567	I	4158.8857	12311.68	14.3103	0.0214	3.0663	9
OH000.453-01.216	P	3640.7034	9728.839	no data			0
OH000.484-00.167	A	142.84	2626.151	11.8193	0	0	3
OH000.517+00.050	A	286.24356	1955.702	12.9859	0	0	3
OH000.580+02.009	A	61.57965	23583.33	9.5278	0	0	3
OH000.621-00.661∗	A	181.54189	14449.86	11.6175	1.4237	135.807	15
OH000.647+01.889	A	249.46605	6658.998	16.292	0	0	1
OH000.667-00.035	P	451.26627	2493745	14.8126	0	0	3
OH000.669-00.056				12.8889	0	0	3
OH000.689+02.140	A	172.24919	4923.821	12.1131	0	0	3
OH000.729+00.451	A	170.91074	4847.505	11.7813	0	0	3
OH000.775-00.282	A	92.341896	30995.39	10.3705	0	0	2
OH000.810-01.959	A	199.28996	5862.393	12.2955	0.031	4.9965	6
OH000.814+00.179	A	142.67366	7983.271	14.1914	0	0	4
OH000.878-03.170	A	138.12457	32450.17	-1.00E+09	error in data		3
OH000.892+01.342	P	1956.313	18739.55	13.3762	0.03792	3.0666	9
OH000.921+02.797	P	820.26733	2757.336	10.094	0	0	3
OH001.072+00.365	P	2485.467	2601.974	11.405	0	0	4
OH001.095-00.832	I	178.85966	1749593	-1.00E+09	error in data		4
OH001.134-00.062	A	701.1178	373.4377	11.506	0	0	5
OH001.155-00.029	F	165.95229	457697.3	7.1924	0	0	2
OH001.184-00.958∗	A	104.69651	6008.719	9.7104	0.9235	141.8219	15
OH001.212+01.257	P	2098.415	28345.48	11.08306	0.4697	3.0667	9
OH001.221+00.294	A	150.63815	4947.753	13.5519	0	0	3
OH001.227+02.005	A	383.29733	10165.76	15.8597	0	0	4
OH001.234+01.273	A	280.3881	4840.88	14.1641	0.01167	3.066025	10
OH001.369+01.003	P	7040.608	173766.6	10.8593	0.02947	3.0663	12
OH001.463-00.997	F	11.912774	144647.7	-1.00E+09	error in data		8
OH001.484-00.061	P	1564.9022	10994.86	no data			0
OH001.604-02.481	A	30.07261	63673.9	-1.00E+09	error in data		1
OH001.611-02.165				14.2473	0.06614	311.1424	10
OH001.628+00.617	F	973.1065	158661.9	13.9707	0	0	2
OH001.794+02.078	P	4442.476	8561.668	12.1301	0	0	3
OH001.803-00.047	P	1907.5424	1433.287	12.2717	0	0	3
OH001.833-01.505∗	A	69.70081	17899.48	9.969	1.2272	200.2445	15
OH001.899-01.953∗	A	61.54629	5449.743	8.7308	1.10389	170.293	7
OH001.908-03.178∗	F	56.37106	113704	8.689	1.1766	314.159	43
OH002.014-02.100	A	30.829863	7516.559	9.5189	0.7824	170.2939	7
OH002.140-00.373∗	A	46.442383	47898.59	10.03107	1.5103	19.5369	10
OH002.186-01.660	P	2607.1338	17533.42	10.5305	0	0	3
OH002.286-01.801	P	2560.4487	16540.06	11.4869	0	0	3
OH002.348+02.965	P	1569.9987	5671.812	11.7448	0	0	3
OH002.360-02.036	A	171.66779	6912.757	8.7974	0	0	3
OH002.362-01.889	F	29.740059	108634.3	-1.00E+09	error in data		1
OH002.382+00.590	A	52.494583	8081.48	9.7583	0	0	3
OH002.582-00.433	F	71.306725	233649.9	-1.00E+09	error in data		2
OH002.640-00.191	P	1082.103	3916.195	13.8822	0	0	4

OH002.642+00.197	A	285.9094	4398.019	no data			0
OH002.721-01.065∗	A	58.88207	8278.594	9.2145	1.689	105.903	16
OH002.726-00.352∗	A	92.22652	3753.325	8.74181.3557	1.3557	75.4056	11
OH003.078-00.027	I	509.79742	6168.824	14.04645	0	0	3
OH003.175-03.024	A	209.19437	6549.72	14.0365	0	0	3
OH003.203+00.024	I	4317.687	1491.661	16.0004	0	0	3
OH003.207+00.675	A	99.490105	9694.739	8.9689	0.529	1.0184	9
OH003.216-00.296	A	168.35829	19246.41	10.6849	0	0	3
OH003.234-02.404	P	1952.5833	7440.406	11.1661	0	0	3
OH003.253-01.468∗	A	56.303696	11823.82	10.2243	1.17581	150.799	10
OH003.289+01.519	A	368.86584	50963.15	9.5653	0	0	2
OH003.304-02.039	P	30551.102	8741.717	9.3356	0	0	3
OH003.471-01.853	P	1153.7671	15682.72	9.7845	0	0	2
OH003.600-02.022	A	325.4395	43234.72	10.7377	0	0	2
OH003.610+00.433	A	185.87448	9086.603	10.3367	0	0	3
OH003.621+00.546	A	64.133705	32620.24	9.5515	0	0	2
OH003.787-01.570	P	1384.9417	1702.669	10.3227	0	0	3
OH003.885-03.085	A	17.082247	8556.258	10.4685	0	0	5
OH003.942-00.008	P	253.0837	17446.66	16.4439	0	0	2
OH003.958-00.537	F	14.852687	197846.7	-1.00E+09	error in data		5
OH004.007+00.915	P	691.12787	8621.814	12.8791	0.01951	4.4928	12
OH004.017-01.679	P	497.71988	6807.355	11.1067	0	0	3
OH004.099-00.631	A	5.446903	36407.17	7.306	0.6138	150.7989	10
OH004.376+00.122	I	228.5131	4363.07	14.3832	0	0	3
OH004.417+00.044	A	85.918495	43651	13.1877	0	0	5
OH004.453+00.129	A	55.83542	7412.528	9.321	0	0	3
OH004.562-00.398	A	40.275032	30471.25	9.1702	1.8777	0.00061	10
OH004.565-00.130	A	56.76615	8262.807	10.8291	0	0	3
OH004.592+01.354	A	200.80775	5831.997	9.4156	0.887	31.0387	16
OH004.680+01.499	P	456.03137	6756.878	16.5948	0	0	3
OH004.887-03.121	P	813.6192	522353.8	-1.00E+09	error in data		1
OH004.961-00.017	A	165.41849	6495.684	12.912	0.1679	31.0387	15
OH005.021-01.724				13.1597	0	0	4
OH005.026+01.491	P	6249.785	4197.284	11.6748	0	0	3
OH005.094-01.528	A	164.72876	69159.75	-1.00E+09	error in data		6
OH005.127+01.490	F	67.33326	128471.1	9.604	0	0	2
OH005.221+00.665∗	A	53.285538	2652.383	11.8814	1.4197	128.7408	8
OH005.417+02.539	A	18.129873	10484.13	9.76181	0.6517	194.725	9
OH005.481+01.066	A	89.7501	42112.8	8.2678	0	0	3
OH005.583-02.345	F	23.139137	191861.5	7.731	0	0	2
OH005.885-00.392	I	219.78746	1403286	11.8958	0.08931	10.9864	9
OH005.987-01.613				12.9214	0	0	3
OH005.991+00.252	F	25.652876	112561.5	7.4939	0.5097	129.7373	4
OH006.095-00.630	A	82.80923	3542.337	15.6578	0.0705	1.9917	12
OH006.235-01.115	A	16.306337	49190.31	7.6874	0.044893	0.9975	11
OH006.236-01.115	A	16.306337	49190.31	7.687	0.0449	0.9975	11
OH006.514-00.171∗	A	109.966064	16937.53	9.5798	0.7692	129.734	10

OH006.594-02.011	A	1451.1982	12123.92	16.4479	0	0	3
OH006.597-01.323	A	101.92725	39870.32	7.2017	0.24211	0.9962	10
OH006.659+01.150	A	299.52182	4500.625	15.5005	0	0	3
OH006.736-00.473	F	40.436024	87471.06	-1.00E+09	error in data		5
OH007.206-01.038	F	45.965027	317423.9	8.1971	1.2153	0.9964	9
OH007.253-01.453	A	41.01886	6937.593	9.1811	0.04696	12.962	11
OH007.307-01.477∗	A	447.1245	35462.73	9.9445	3.7755	14.9537	4
OH007.420-02.042	A	1399.1497	24666.47	16.3257	0	0	2
OH007.452-02.615	A	1096.3533	68675.28	no data			0
OH007.542-00.056	A	52.719486	66416.53	9.6094	0.3231	49.8798	9
OH007.885+00.240	F	2687.1191	129893.9	9.224	0.01149	49.8798	9
OH007.958-00.393	A	17679.957	2836.489	14.4608	0.04516	12.9513	8
OH007.961+01.445	P	1831.9711	37800.65	13.4058	0	0	3
OH008.328-01.802∗	A	41.498398	29112.04	10.7613	1.0418	120.7845	9
OH008.328-01.803∗	A	41.498398	29112.04	10.7613	1.0418	118.8919	9
OH008.344-01.002	F	133.95728	7383441	no data			0
OH008.483+00.176				8.929	0.4692	31.0912	10
OH008.533+00.108∗	A	191.58733	15160.5	10.1857	4.1581	80.0024	9
OH008.707+00.811	P	1085.547	17551.07	13.4802	0	0	4
OH008.733+00.549	P	625.31604	4621.642	15.2255	0.3892	80.9711	14
OH008.854+01.689	P	1443.3619	16355.22	11.4152	0	0	3
OH008.885-00.516	A	234.04279	4115.756	13.4008	0	0	3
OH008.885-00.517	A	234.04279	4115.756	13.4008	0	0	3
OH008.933-00.014	F	115.46116	2320474	-1.00E+09	error in data		2
OH008.933-00.015	F	115.46116	2320474	-1.00E+09	error in data		2
OH008.952-00.045	A	18.057522	8412.081	no data			0
OH008.991-00.140	A	192.11783	1589.941	15.8012	0	0	2
OH009.055-00.156	P	158.50818	13228.69	no data			0
OH009.056-00.156	P	158.50818	13228.69	12.3644	0	0	3
OH009.097-00.392	P	979.57043	9010.881	no data			0
OH009.133-00.524	A	197.16963	17906.44	13.2432	0	0	3
OH009.334+00.129	F	19.65005	444229.5	7.0185	0	0	3
OH009.335+00.129	F	19.65005	444229.5	7.0185	0	0	3
OH009.341-00.570	A	438.68982	2951.844	13.6532	0	0	3
OH009.375-01.308	P	87.97778	5815.485	13.6989	0	0	3
OH009.475+02.014	A	49.01121	11036.51	11.2028	0	0	1
OH009.574-02.032	F	27.615896	81859.66	no data			0
OH009.575-02.032	F	27.615896	81859.66	no data			0
OH009.630+00.496	A	20.992395	19894.77	7.5899	0	0	2
OH009.877-00.128	A	49.37141	9931.03	9.7543	0	0	6
OH009.878-00.128	A	49.37141	9931.03	9.7543	0	0	6
OH350.202-00.757	P	1290.1166	20885.59	15.113	0.05896	165.6905	9
OH350.287+00.058	P	271.54388	9643.016	12.9725	0	0	3
OH350.350-02.372				14.5483	0.01067	13.9749	8
OH350.384-00.425	P	249.83563	6430.564	11.62	0.2393	165.6904	8
OH350.494+02.394	A	244.17783	12027.79	14.6229	0.2792	62.8881	9
OH350.546+00.061	I	4857.5854	5909.886	15.5487	0	0	4

OH350.749+02.898	A	34.29985	77989.18	7.1887	0	0	7
OH350.815-01.433∗	A	107.83421	35732.58	9.3152	1.8476	82.8447	6
OH350.836+02.106	F	32.602604	199694	7.1953	0	0	6
OH350.848+00.184	P	6779.347	25895.24	13.6876	0	0	4
OH350.982-02.391	F	48.400173	85333.07	7.323	0	0	1
OH351.118-00.352	P	528.1165	16051.36	15.5758	0.1281	154.7485	9
OH351.142+00.068	P	1262.5731	5232.772	11.9534	0	0	3
OH351.219+00.259	A	1155.2455	826.9854	14.0322	0	0	3
OH351.315-00.010	A	77.99298	10862.61	no data			0
OH351.361-02.004	A	37.786507	7996.426	9.9658	0.0459	13.9747	8
OH351.474-00.596	I	626.24066	6604.061	11.5618	0.04071	82.8495	18
OH351.486+03.263	A	181.5475	4307.76	no data			0
OH351.526+02.502	A	143.94585	15941.94	no data			0
OH351.592+00.318	P	288.7365	5747.65	17.071	0	0	1
OH351.607+00.022	A	64.10873	45399.5	11.3093	0.1436	84.785	9
OH351.774-00.536	P	221.47931	1237149	16.0.0230	0.023	79.3467	4
OH352.044+00.530	A	34.442135	76421.71	9.2954	0.0691	23.8428	9
OH352.135-01.369∗	F	97.60513	234798.8	8.2532	1.989	79.3466	7
OH352.554-01.941	A	23.089855	63802.76	8.6921	0	0	3
OH352.616-00.195	F	183.5919	103226.8	9.25	0.0621	23.8426	9
OH352.625+03.014	F	101.97673	2.34E+07	no data			0
OH352.749-00.644	A	64.94658	31793.61	9.071	0.1195	158.6927	15
OH352.888-03.033	P	293.38007	16052.09	10.5846	0	0	3
OH353.037-02.457	A	151.35599	1499.425	13.2961	0.1194	17.0039	8
OH353.136+00.082	A	539.017	5227.207	15.5937	0.1371	80.7946	9
OH353.298-01.537	P	219.80939	18494.71	13.0279	1.075	162.6226	14
OH353.536+00.605	P	2358.2434	2924.988	10.5001	0.1207	76.7331	8
OH353.573+00.455	A	219.13809	27538.57	7.6153	0.2224	4.062	3
OH353.574+00.598	P	801.3006	4036.463	10.9395	0.0096	4.0621	9
OH353.607-00.236	A	188.5956	80417.53	8.4973	0.958	4.062	8
OH353.637+00.815	P	748.0581	15886.21	14.3088	0.07615	88.35	16
OH353.747-01.541∗	A	61.807095	23168.16	8.7652	2.3652	26.949	11
OH353.810+01.452	F	528.68726	271300.1	7.6248	0	0	1
OH353.843-02.633	A	5.867113	75277.95	7.305	0	0	6
OH353.844+02.984	P	59861.57	461148.3	no data			0
OH353.945-00.972	P	9644.914	10107.98	11.29	0.0991	66.9407	12
OH353.973+02.727	P	884.3069	9667.793	no data			0
OH354.104-01.982	F	85.42049	99809.84	1.00E+09	error in data		1
OH354.415+00.112	A	98.97461	9573.644	9.83	0.3459	76.7382	10
OH354.509-01.377	I	11927.961	5297.883	12.2057	0.05874	13.4687	12
OH354.529+00.038	A	396.85876	9575.639	10.1621	0.1786	76.7384	9
OH354.601+00.244	A	100.01222	4120.635	12.5015	0.4267	80.7998	9
OH354.642+00.830	P	250.60767	3316.75	14.9957	0.0828	99.846	12
OH354.647-00.182	I	1039.7286	28976.92	9.2057	0.2762	80.8011	10
OH354.762-00.062	P	260.23883	22015.77	13.9955	0.9825	80.7992	9
OH354.776-00.277				11.8556	0.03695	4.061	12
OH354.884-00.539	P	117.51395	968395.6	13.835	1.5202	66.9293	16

OH354.968-01.066∗	A	89.80208	27890.6	12.3549	0.9382	66.9296	12
OH355.021+00.146	P	241.50844	27737.4	8.8444	1.2001	4.06092	7
OH355.091-00.954	A	286.06546	3840.053	11.5832	0.02936	39.9923	10
OH355.111-01.697	I	41865.918	7061.351	9.4606	0.3912	17.0041	6
OH355.156-00.597	F	58.921745	530835.1	no data			0
OH355.355-00.014∗	A	212.68501	3986.664	14.1348	5.04965	38.9111	9
OH355.401-01.596	P	2044.3848	1445.066	9.276	0.0214	17.0045	4
OH355.435+00.597	A	270.37506	19939.15	10.5637	0.5325	76.7388	9
OH355.488+02.886	A	125.904686	32380.55	no data			0
OH355.588-02.978	F	140.49252	799314.4	no data			0
OH355.641-01.742	P	1099.903	5626.538	9.103	0.2314	17.0045	6
OH355.651-03.231	A	821.68463	4588.801	9.7193	0.364	17.0043	6
OH355.815-00.226	A	1760.2919	12919.42	14.2033	0.1402	76.7387	9
OH355.863-02.985	F	23.186909	976687.6	-1.00E+09	error in data		3
OH355.897-01.754	A	125.49135	32687.51	11.145	0.1352	6.5346	9
OH355.914-01.126	A	48.671318	11496.24	7.9063	0.1787	26.041	11
OH356.273-03.018	A	16038.506	41941.06	-1.00E+09	error in data		7
OH356.373+00.297	A	336.5143	12634.17	no data			0
OH356.501-00.549	P	58.984375	6705.411	11.4962	0.1936	26.0412	12
OH356.524+02.526				13.2936	0.0172	115.7699	5
OH356.562-02.527	P	5495.093	8829.044	9.3067	0.3238	6.5331	9
OH356.591-01.428				14.4192	0.05913	26.041	12
OH356.631+00.409	A	29.716938	43000.47	7.1542	0	0	2
OH356.646-00.153	A	525.04535	4579.931	no data			0
OH356.662+00.113	A	64.2252	2724.917	11.1399	0.0339	3.9666	6
OH357.092-00.362	P	1541.564	3686.357	12.1554	0.1475	87.86	14
OH357.146-00.750	F	16.541702	440198.6	7.2142	0	0	3
OH357.149-01.009∗	A	28.016548	2604.669	10.9161	1.5111	142.8331	12
OH357.180-00.521	A	961.29266	3953.315	12.5103	0.02144	26.0411	12
OH357.301+02.893	A	135.16089	4748.515	10.4055	0.0404	116.7599	10
OH357.311-01.337	F	123.34301	4949961	13.8548	0.6601	142.8331	22
OH357.393-02.779	P	3701.3213	4586.154	9.7815	1.6121	64.3257	11
OH357.474+00.367	P	1458.6267	3598.82	11.4741	0.0056	3.9702	10
OH357.609-00.188	F	16.244001	168611.3	7.5099	0.1048	3.9702	4
OH357.638+01.890	A	59.42701	2987.736	10.7094	0	0	3
OH357.675-00.060	A	63.584167	11444.3	10.7094	0.0696	3.9702	6
OH357.711-00.270	P	207.60791	56328.16	7.851	0.0938	3.9702	7
OH357.749+00.320	P	1926.0537	6793.976	13.3951	0.0229	3.9702	6
OH357.819+01.990	A	109.90449	28130.92	11.2331	0	0	3
OH357.980+00.826	P	1212.2385	2057.203	10.5882	0.07495	7.096	9
OH357.988-00.988	A	208.26674	5988.71	16.3262	0.4565	26.03	12
OH358.039-01.684	P	1855.9551	2657.641	9.9709	0.0316	6.524	15
OH358.052+01.304	A	125.74265	8105.382	13.6372	0.0185	3.5449	9
OH358.083+00.137	P	1509.9945	981.7109	11.9298	0.0171	3.9702	6
OH358.162+00.490	F	37.073063	1016113	-1.00E+09	error in data		1
OH358.236-02.659	F	66.9535	147671.2	7.3862	0.1096	26.9667	6
OH358.273-00.665∗	A	276.37622	2681.388	14.5107	0.8559	26.03	13

OH358.366+02.805	A	473.6805	17714.6	8.9275	0	0	3
OH358.422+00.238	A	12.19376	41249.02	7.635	0.2313	3.9698	5
OH358.425-00.175	P	1161.6041	10574.2	12.3695	0.0404	3.9706	6
OH358.436+00.442	F	27.889656	836202.7	-1.00E+09	error in data		5
OH358.478-02.916	A	292.24277	6278.781	9.8749	0.1957	77.8093	12
OH358.497-00.081	F	98.03212	226376.8	no data			0
OH358.497-02.952	F	54.21386	87511.74	11.0318	0.6903	77.8092	12
OH358.505+00.330	P	3627.3438	7247.057	9.3667	0	0	5
OH358.522-01.061∗	A	97.44355	6583.614	11.9598	1.1743	116.794	12
OH358.649-01.701	A	188.95033	37357.43	9.379	0.2153	13.0475	9
OH358.667-00.044	F	38.589523	916668.1	no data			0
OH358.720-00.620	A	30.085466	13458.66	8.1287	0.6762	71.4119	9
OH359.011-00.116	A	515.96844	2110.149	12.5396	0	0	1
OH359.033+01.938	P	431.7964	5186.386	no data			0
OH359.069-01.327	F	13.680358	174191.8	-1.00E+09	error in data		7
OH359.117-00.169	A	139.5367	10285.81	12.2334	0	0	5
OH359.140+01.137	P	995.6614	7209.504	10.5488	0.234	7.0914	9
OH359.147+01.023	A	2423.9717	16983.06	9.7816	0.0466	3.545	8
OH359.149-00.043	A	25.634657	37198.22	12.0824	0	0	1
OH359.161-00.055	A	412.6578	8530.856	12.2087	0	0	2
OH359.201+00.285	A	550.9738	3507.21	12.5831	0	0	4
OH359.220+00.163	P	1360.9418	1421.605	11.9257	0	0	3
OH359.233-01.876	I	3767.227	15074.1	11.8085	0.0397	54.3336	12
OH359.360+00.084	A	263.62735	2662.892	14.7571	0	0	3
OH359.380-01.201	P	1937.3035	10520.29	11.8076	0.4294	57.9807	39
OH359.429+00.036	P	605.82556	1950.741	12.9788	0	0	3
OH359.467+01.029	A	208.4499	4924.783	12.5412	0.06157	3.5459	9
OH359.486-02.942	A	2914.5571	26549.11	10.9509	0.5838	57.8238	12
OH359.499-03.302	P	4257.004	24922.11	13.3022	0.0251	54.3317	14
OH359.500+02.776	P	132.63983	9406.889	no data			0
OH359.543-01.775	A	21368.73	15228.24	9.7156	0.3499	54.3337	12
OH359.564+01.287	A	323.9633	4905.954	12.8257	0.0853	7.0913	9
OH359.581-00.240				11.9141	0	0	3
OH359.632-00.431	A	94.487495	6338.09	13.0429	0.6626	136.7073	28
OH359.664+00.636∗	A	221.59962	5361.6	9.2803	1.9887	121.748	8
OH359.731+01.260	P	89.49011	3695.082	13.0801	0.148	7.0914	9
OH359.745-00.404	A	121.25097	4676.909	12.1205	1.7619	142.7202	28
OH359.750+02.629	P	1947.0975	13050	no data			0
OH359.751+00.607	A	216.22243	2876.091	11.1063	0	0	3
OH359.762+00.120	F	90.182304	82010.31	no data			0
OH359.783-00.391	A	161.33981	3360.283	12.5915	0.1839	77.9247	28
OH359.857+01.005	A	67.627716	4409.77	11.558	0.03548	7.0913	18
OH359.872-01.488∗	A	147.33485	5065.525	7.6384	2.372	31.7991	26
OH359.938-00.052	I	770.2706	5736653	12.4176	0	0	3
OH359.938-00.077				12.2229	0	0	3
OH359.946+01.593	F	355.1741	262570.9	6.4351	0	0	5
OH359.952-00.035				14.166	0	0	1

OH359.954-00.041				no data		0
OH359.978+02.563	F	36.242855	201891.4	no data		0
OH359.985-00.061	A	130.63316	32746.82	10.1911	0	

6 Acknowledgement

This publication makes use of VOSA, developed under the Spanish Virtual Observatory project supported from the Spanish MICINN through grant AyA2008-02156.

This publication also made use of The ALADIN interactive sky atlas. A reference tool for identification of astronomical sources. Bonnarel F.; Fernique P.; Bienayme O.; Egret D.; Genova F.; Louys M.; Ochsenbein F.; Wenger M.; Bartlett J.G.

References

[1] Engels, Dieter. *AGB and post-AGB stars*, arXiv preprint astro-ph/0508285 (2005).

[2] Olofsson, Hans. *The AGB-star Phenomenon: Setting the Stage*, Asymptotic Giant Branch Stars **191** (1999), 3.

[3] Sevenster, MN and Van Langevelde, HJ and Moody, RA and Chapman, JM and Habing, HJ and Killeen, NEB. *The ATCA/VLA OH 1612 MHz survey*, A&A **366** (2001), 481–489.

[4] Sevenster, MN and Chapman, JM and Habing, HJ and Killeen, NEB and Lindqvist, M. *The ATCA/VLA OH 1612 MHz survey. II. Observations of the galactic Disk region*, Astronomy and Astrophysics Supplement Series **124** (1997), 509–515.

[5] Sevenster, Sevenster, MN and Chapman, JM and Habing, HJ and Killeen, NEB and Lindqvist, M. *The ATCA/VLA OH 1612 MHz survey. I. Observations of the galactic bulge Region*, Astronomy and Astrophysics Supplement Series **122** (1997), 79–93.

[6] Wright, Edward L and Eisenhardt, Peter RM and Mainzer, Amy K and Ressler, Michael E and Cutri, Roc M and Jarrett, Thomas and Kirkpatrick, J Davy and Padgett, Deborah and McMillan, Robert S and Skrutskie, Michael and others. *The Wide-field Infrared Survey Explorer (WISE): mission description and initial on-orbit performance*, The Astronomical Journal **140** (2010), 1868.

[7] Churchwell, Ed and Babler, Brian L and Meade, Marilyn R and Whitney, Barbara A and Benjamin, Robert and Indebetouw, Remy and Cyganowski, Claudia and Robitaille, Thomas P and Povich, Matthew and Watson, Christer and others. *The Spitzer/GLIMPSE surveys: a new view of the Milky Way*, Publications of the Astronomical Society of the Pacific **121** (2009), 213–230.

[8] Egan, MP and Price, SD and Kraemer, KE and Mizuno, DR and others, *MSX6C Infrared Point Source Catalog*, The Midcourse Space Experiment Point Source Catalog Version **2** (2003).

[9] Beichman, CA and Neugebauer, G and Habing, HJ and Clegg, PE and Chester, Thomas J. *Infrared astronomical satellite (IRAS) catalogs and atlases. Volume 1: Explanatory supplement*, Infrared astronomical satellite (IRAS) catalogs and atlases. Volume 1: Explanatory supplement **1** (1988).

[10] Ishihara, Daisuke and Onaka, Takashi and Kataza, Hirokazu and Salama, Alberto and Alfageme, Carlos and Cassatella, Angelo and Cox, Nick and Garcia-Lario, Pedro and

Stephenson, Craig and Cohen, Martin and others. *The AKARI/IRC mid-infrared all-sky survey*, arXiv preprint arXiv:1003.0270 (2010).

[11] Yamamura, Issei. *The AKARI Far-Infrared Bright Source Catalogue*, 38th COSPAR Scientific Assembly **38** (2010), 2496.